**J. Build. Mater. Struct. (2025) 12: 49-62** *Original Article*
DOI : 10.34118/ jbms.v12i1.4139

# Revolutionizing Rigid Pavements Towards Magnetizable Concrete Materials for Charging Electric Vehicles

Mohamed Abdel Raouf [1*], Yassien Zidan[2], Hana Alnaas [2], Rand Abo ElEnain [2], Abdullah Mahmoud [2], Mahmoud Seddik [2], Mayar Mohamed Khairy [2], Mohamed Nagib Abou-Zeid [2]

1 Ball State University, Department of Construction Management and Interior Design, 2000 W. University Avenue, Muncie, IN 47306, USA.
2 The American University in Cairo, Department of Construction Engineering and Management, AUC Avenue, New Cairo 11835, Egypt.
* Corresponding Author: maraouf@bsu.edu

**Received: 20-02-2025** **Accepted: 24-05-2025**

**Abstract.** Nowadays, the green economy dictates the urge for finding innovative construction materials to be compatible with the future needs. The growing potential of electric vehicles (EVs) necessitates the transformation towards sustainable and magnetizable concrete pavement. The primary objectives of this work are to determine the optimal materials and mixing proportions to produce high-performance magnetizable mortars for pavement applications. The experimental testing program includes assessing the magnetic properties through the inductance test, the fresh properties using the mini-slump test, the hardened properties through the compressive strength at 3, 7, and 28 days, and the durability through chemical soundness and abrasion resistance. It may be concluded that the magnetic properties of Portland cement mortars can be enhanced through the incorporation of natural magnetite (25% replacement), slag (25% replacement), and scrap iron fillings (70% replacement), and importantly, the addition of enhancers such as magnets, steel mesh, and/or steel bars. These magnetizable mortars can be used for rigid pavement applications since they have a higher abrasion resistance.

**Key words:** Magnetizable Concrete, eRoads, Smart Pavements, Recyclable Materials.

## 1. Introduction

With the significant expansion in road traffic volumes and the prevalence of fuel-based vehicles, the air quality issues have been exacerbated. This has prompted numerous transportation agencies and corporations to address the increasing needs and demands of road users. Hardman et al. (2021), among many others, assert that the promotion of electric vehicles (EVs) introduces profound environmental benefits including the reduction of $CO_2$ emissions, the mitigation of climate change, and the decrease of air pollution (International Energy Agency, 2023). These advantages stem from replacing traditional internal combustion engines, which rely on fossil fuels, with electric motors powered by chargeable batteries.

By 2030, based on an estimate by the International Energy Agency (IEA), there will be 250 million EVs on the roads worldwide, with an average of 44 million sold each year, and this is mainly due to the growing investment in manufacturing zero-emission cars by the automotive industry (IEA, 2023). According to the IEA report and analysis of EVs sales data in 31 counties, limited driving range seems to be the largest barrier to EV ownership. However, some EV owners argue that the purchasing price is also a significant limitation (Hardman et al., 2021). Therefore, the issue of battery time range plays a crucial role in the promotion of these EVs. Specifically, 81% of US drivers were concerned about wireless charging, and 70% were prepared to buy an EV if wireless charging were available (IEA, 2023).

After the convention of magnetic resonance coupling by Nikola Tesla in the 19th century, wireless power transfer (WPT) is being widely adopted and used by many other applications and electronic devices (Bhagyashree et al., 2023). According to Reza Tavakoli et al. (2017), WPT is a safe and convenient way to transfer tens of kilowatts of power between the stationary transmitter pad and a stationary or moving vehicle (Seixas Esteves et al., 2022). The development of the charging process, specifically inductive wireless charging, in the past few years led to the increasing number of electric vehicles in the automotive industry (Car and Drivers, 2017). For example, automobiles manufacturers such as Mercedes-Benz, BMW, and Hyundai are in the process of incorporating inductive charging systems into their EV models, allowing for hands-free operation and enhanced charging efficiency (Car and Drivers, 2017). Thus, the evolution of wireless charging for EVs is recognized as a key enabling technology for autonomous driving, creating huge opportunities for policymakers, state agencies, fleet owners, automakers, and original equipment manufacturers to work together toward diverse EV models and widespread adoption of EVs. In addition, wireless charging for EVs has three different techniques that can be listed as follows: (a) static while parking, (b) semi-/quasi-dynamic while deaccelerating/accelerating from a stationary position, and (c) dynamic charging while moving (Tiemann et al., 2020).

Nowadays, there are many projects, whether existing or under construction, that prove that wireless dynamic charging for electric vehicles is a practical way to promote wireless charging for can be summarized as follows: First, in 2013, two On-Line Electric Vehicle buses developed by the Korea Advanced Institute of Science and Technology were able to charge through wireless sections of road in Gumi, South Korea. Second, in 2017, Qualcomm successfully charged a fleet of specially modified Renault Kangoo electric vans, each fitted with two 10 kW charging pads and traveling at a speed of 70 mph, through its hardware capable of wireless power transfer on a 100-meter test track. Third, Electron has built the USA's first public electric roads in Detroit, Michigan, in 2023, in partnership with Ford Motor Company, where electric cars, trucks, and buses can charge their batteries while traveling along this one-mile-long electrified road of the downtown.

However, standards are essential for the wider acceptability of any new technology. Evaluation of the design and construction of electrified roads (eRoads) adopting WPT is crucial to be conducted for better enhancement of eRoads and in view of charging module elements and lane arrangement, structural capacity, construction processes, maintenance requirements, and performance (Reza Tavakoli et al., 2017). Under the Society of Automotive Engineer "SAE" leadership, the Cooperative Research Project (CRP), including leading automotive and power electronics industries such as BMW, Ford, General Motors, Honda, IHI, Qualcomm, WiTricity, etc., is formed for additional vehicle and emissions testing using industry-committed funds. In the future, the SAE J2954 Taskforce will be working on higher-power WPT technology with SAE J2954/2 for buses and heavy-duty vehicles (Schneider et al., 2018).

In this study, literature review coupled with analysis were conducted to better understand the nature and properties of materials and techniques used for enhancing the magnetic properties of portland cement mortars. Therefore, this complete desktop research was conducted based on reliable and well-established academic databases such as Scopus since it is the most commonly used research engine and because most of the references are already registered within its database. It was found that the best keywords to be used in this research was wireless charging concrete with some limitations as the search query below. The results was only 10 papers found from 2017 to 2024. After that, to guarantee the inclusion of the most pertinent and recent research, the abstract of these papers was read and then filtered according to parameters such as subject matter, specialization of journals, and date range.

**Search Query:** TITLE-ABS-KEY (wireless AND charging AND concrete) AND (LIMIT-TO (SUBJAREA, "ENGI")) AND (LIMIT-TO (EXACTKEYWORD, "Concretes")) AND (LIMIT-TO (LANGUAGE, "English"))

The investigation of the materials and constituents influencing magnetic properties of portland cement mortars and concrete was made by this methodical approach. It may be concluded that very limited number of papers were focused on the materials suitable for enhancing the magnetic permeability of concrete and the corresponding mixture design. The magnetic permeability of concrete is a parameter to assess how easy it is for the magnetic flux to pass through the concrete materials, and it is an indication of the formation of magnetic fields within concrete material itself. On the other hand, magnetic conductivity is the ability of the material to allow for the magnetic energy to pass through it. Therefore, magnetic permeability and conductivity are indirectly related to each other, but the most used term is the magnetic permeability. However, few research studies have shown that incorporating magnetite into cement mortar and concrete can enhance its mechanical and magnetic properties, including compressive strength. Additionally, studies have indicated that utilizing the low-cost natural magnetite can boost the effectiveness of wireless charging systems due to its low electrical conductivity and hysteresis (Yaowen et al., 2023).

Portland cement is a low-cost binder and weakly ferromagnetic due to the low traces of ferrous iron oxide, which increase magnetic permeability. Calcium silicates account for approximately 75% of the cement composition, and after the cement is hydrated, most of the products, though primarily calcium-based, have both crystalline calcium hydrate (CH) and amorphous calcium silicate hydrate (C-S-H). Therefore, it may be concluded that these materials are responsible for the strength of concrete and are the reasons that concrete poses low magnetic permeability properties. There are many low-cost materials and additives with high magnetic permeability were investigated to enhance concrete and mortar properties, such as natural magnetite, synthetic magnetite and steel filings (Bhagyashree et al., 2023). The inclusion of additional ferritic material is necessary to attain the levels of permeability required to positively enhance the efficiency of the wireless power transfer device and provide structural protection. Recent studies have been emerging into two main directions that can be listed as follows: (a) incorporating permanent magnets into road constructions; and (b) mixing magnetic powders with conventional pavement materials to prepare magnetic pavement materials (Soares, 2022). According to Reza Tavakoli et al. (2017), magnetic composite materials consist of two basic parts: (a) magnetic fillers of specific size, shape, and volumetric ratio that determine the magnetic properties of the composite; and (b) a matrix that controls the homogeneity of magnetic particles in the composite and significantly affects the non-magnetic and mechanical properties of the composite materials.

This type of rich-iron mortars will not be globally accepted as a building and construction materials without reliable and extensive data regarding its long-term properties. In this study, the focus was on chemical attach and abrasion resistance since the main usage will be in road applications. Since the usage of steel rebars is high possibly in these road applications mortars and concretes, it is paramount at later stages to study other long-term properties of these iron-rich mortars for better operational and maintenance practices. Based on literature review, many reinforced concrete structures fail before reaching the end of their service life (Glass et al., 2000 and Tang et al., 2015). Specifically, steel corrosion is one of the main reasons for premature failure of reinforced concrete structures (Glass et al., 2000 and Tang et al., 2015).

Also, the durability of iron-rich mortars with high content of ferrous compositions should be assessed thoroughly. The long-term properties may be addressed by studying many parameters such as corrosion behavior, permeability, chemical soundness (sulfate and chloride attacks), alkalinity (pH values), overall stability, fire resistance, chemical composition, microstructure, and excessive vibration. Importantly, corrosion affects significantly the long-term properties of structures, such as load-carrying capacity and serviceability that lead to major safety issues. Specifically, the corrosion behavior of these iron-rich mortars needs to be investigated to determine the long-term impact on compressive strength, volumetric stability, thermal stress, permeability, carbonation of portland cement, and chloride-induced corrosion.

## Work Objectives

This study is an attempt to improve the understanding of magnetic properties of magnetizable portland cement mortars and seeking means to produce cementitious materials that possess magnetic properties. The key sequential objectives were achieved through the following methodology;

A. To conduct a systematic desktop literature review on magnetizable concrete and mortar including recent research development.

B. To evaluate the most suitable materials to be incorporated in magnetizable mortar.

C. To determine the appropriate percentage of these selected materials to enhance the mortar's magnetic performance.

D. To assess the magnetic properties of portland cement mortars and subsequently evaluate the fresh and hardened properties of the mixture that demonstrates the near-optimum magnetic properties.

## 2. Experimental program

### *2.1. Materials*

Cement: type I ordinary portland cement that has a specific gravity of 3.16 and a specific surface area (Blaine fineness) of 375 $m^2/kg$ was used.

Fine Aggregates: siliceous river sand that has a fineness modulus of 2.88, a saturated surface-dry specific gravity of 2.51, and an absorption of 0.50 percent was used.

Water: typical municipal tap water was used.

Slag: ground granulated blast furnace slag, featuring a specific gravity of 2.90 and a Blaine fineness of 400 $m^2/kg$, was used. The slag was used as a cement replacement in different percentages.

Magnetite: natural magnetite aggregate with a specific gravity of 5.15 was used, as shown in Figure 1(a).

Synthetic magnetite: this can be manufactured in chemistry laboratories according to the following procedure:

a) $FeCl_3$ and $FeCl_2$ are gathered with a 2:1 ratio.

b) This gathered material reacts with 10% NH4OH at 40–80 °C.

c) The resulted compound is stirred with a rate of 300–500 rpm in a beaker glass.

d) The final compound, after stirring, is precipitated and dried in the oven at 100 °C.

Steel bars: steel reinforcement bars with a diameter of 8 mm and a specific gravity of 7.85.

Stainless steel wire mesh: a mesh made from stainless steel, characterized by its corrosion resistance and a wire diameter typically around 0.5 mm.

Scrap iron fillings: fine scrap recyclable iron filings, as shown in Figure 1(b), with a specific gravity of 7.87, were used as a fine aggregate replacement to enhance the magnetic properties of the mortar. This was supplied by a local supplier.

Neodymium Magnet: Neodymium magnets were incorporated to enhance the magnetic responsiveness of the mortar (Figure 1 (c)). These recyclable magnets have a high residual magnetism and a specific gravity of 7.5.

**(a) Magnetite** **(b) Scrap Iron Fillings** **(c) Neodymium (40x20x10 mm)**

**Fig 1. Materials Used in Cement Mixtures**

## *2.2. Mixture Design and Experimental Phases*

Given the current gap in knowledge regarding the properties and proportions of constituent materials necessary for achieving adequate magnetizable properties, this study has undertaken extensive preparatory trials, divided into three main phases with 17 mixtures having different constituents. These efforts have been pivotal in refining the proportions and parameters, ultimately aligning them with the study's objectives. As illustrated in Table 1, the study was conducted in three sequential phases:

i. Phase A that focused on the usage of a single constituent in cement mortar with quite low percentages.

ii. Phase B that involved the simultaneous usage of two constituents in small percentages within the mixtures.

iii. Phase C that incorporated two or three constituents at high percentages along with the addition of various enhancers. In phase C, all the constituents were fixed; all four mixtures contained the same proportions of constituents, 25% magnetite, 25% slag, and 70% iron fillings, while differing only in the enhancers utilized.

Magnetizable Portland cement mortar mixtures were prepared with a water-to-cementitious materials ratio (w/cm) of 0.48, chosen for its moderate and commonly used ratio in Portland cement mortars and concrete. The mixtures included varying percentages of magnetite, replacing fine aggregates at levels of 4%, 30%, 40%, and 70%, as shown in Table 1. Slag was incorporated as a binding agent, replacing Portland cement at proportions of 10%, 15%, and 25% by weight. Moreover, scrap recyclable iron filings were added, replacing fine aggregates at proportions of 10%, 15%, and 25%; to enhance the magnetic properties of the mixtures. High magnetic property materials, referred to as enhancers, were also added, including: (a) steel bars with a diameter of 8 mm; (b) steel mesh with a diameter of 0.5 mm; and (c) neodymium magnets.

## *2.3. Experimental Testing*

### *2.3.1. Inductance Test*

The inductance test was conducted in accordance with ASTM A772, following the setup illustrated in Figure 2. This test is vital for evaluating the mortar's interaction with magnetic fields. The testing procedure was designed to measure the current versus voltage (I-V) characteristics of various mortar mixtures, aiming to assess how magnetic materials enhance the conductivity and magnetic properties of cement mortars. The samples were cubic, with dimensions of 40x40x70 mm, as indicated by the green circle in Figure 2. During testing, the measured parameters included current in amperes (Amp) and voltage in volts (V), while the calculated parameters were inductance in Henry (H) and magnetic permeability ($\mu$) in Henry/meter (H/m).

**Table 1. Mixtures of cement mortars in phases A, B, and C**

| Phase | Mixt-ure ID | Constituents | | | | | | Enhancers | | |
|---|---|---|---|---|---|---|---|---|---|---|
| | | Water (g) | Slag (g) (%) | Magnetite (g) (%) | Iron Fillings (g) (%) | Cement (g) | Fine Aggregates (g) | Magnet | Steel Bars | Mesh |
| A | I | 726 | 0 | 0 | 0 | 1,500 | 4,125 | - | | |
| | II | | 150 (10) | 0 | 0 | 1,350 | 5,500 | | | |
| | III | | 225 (15) | 0 | 0 | 1,275 | 5,500 | | | |
| | IV | | 0 | 165 (4) | 0 | 1,500 | 3,960 | | | |
| | V | | 0 | 1,238 (30) | 0 | 1,500 | 2,887 | | | |
| | VI | | 0 | 2,888 (70) | 0 | 1,500 | 1,238 | | | |
| | VII | | 0 | 0 | 413 (10) | 1,500 | 3,712 | | | |
| | VII | | 0 | 0 | 619 (15) | 1,500 | 3,506 | | | |
| | IX | | 0 | 0 | 1032 (25) | 1,500 | 3,093 | | | |
| B | X | | 375 (25) | 0 | 25 | 1,125 | 4,125 | - | | |
| | XI | | 375 (25) | 0 | 40 | 1,125 | 3,300 | | | |
| | XII | | 150 (10) | 40 | 15 | 1,350 | 2,475 | | | |
| | XIII | | 225 (15) | 40 | 15 | 1,275 | 2,475 | | | |
| C | XIV | | 375 (25) | 2,888 (70) | 1,031 (25) | 1,125 | 206 | ✓ | - | - |
| | XV | | | | | | | - | ✓ | - |
| | XVI | | | | | | | - | - | ✓ |
| | XVII | | | | | | | ✓ | ✓ | - |

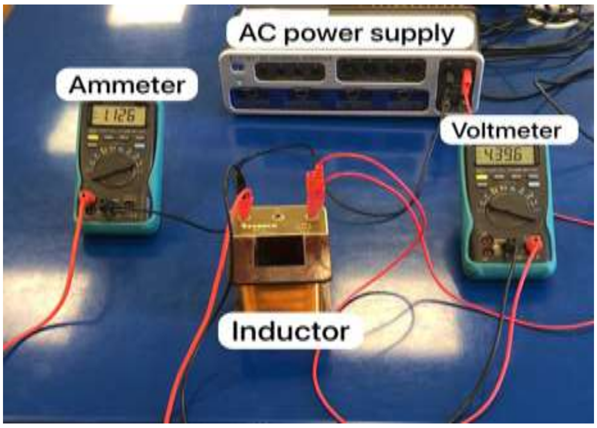


**Fig 2. Inductance test set up**

### *2.3.2. Mini-Slump*

The mini-slump test was conducted using a non-standardized method to evaluate the mortar's workability. The guidelines followed for this test were adapted from ASTM C1437, which covers the flow of hydraulic cement mortars, which pertains to fresh mortar tests. The primary parameter measured was the diameter of the spread to assess the flowability of the cement mortar mixture, categorized as high (200-300 mm), medium (150-200 mm), low (100-150 mm), or viscous (less than 100 mm).

### *2.3.3. Compressive Strength*

The compressive strength of various cement mortar mixtures was measured according to ASTM C109 at 3, 7, and 28 days.

### *2.3.4. Durability*

The durability of different mixtures was assessed through abrasion resistance, conducted in accordance with ASTM C1803, to determine the wear resistance of the mortar. Additionally, chemical attack testing was performed following ASTM C267 to assess the mortar's ability to withstand harsh chemical environments. These tests were essential for assessing the mortar's durability for construction applications and its suitability for wireless power transfer applications.

## 3. Results and discussion

After finalizing the mixture design, the experimental testing phases commenced. Initially, testing related to the mixtures' magnetic properties was conducted in Phase A, followed by Phases B and C. Subsequently, certain selected mixtures were assessed for their fresh and hardened properties.

### *3.1. Magnetic Properties*

### *3.1.1. Inductance Test*

Figure 3 illustrates the current versus voltage (I-V) behavior for the air sample and iron bar, which are used as reference benchmarks for subsequent comparisons. These reference materials serve to establish a baseline for evaluating the magnetic properties of other mixtures. Mixtures with current versus voltage (I-V) characteristics that are closer to those of the iron bar are deemed to exhibit superior magnetic properties compared to those nearer to the air sample.

Data For Air core and Iron core for Inductance test

| | ▲ Set | ■ Air Core | ● Iron Bar Core |
|---|---|---|---|
| | Voltage (v) | Current (A) | Current (A) |
| 1 | 0.5 | 0.126 | 0.030 |
| 2 | 1.0 | 0.256 | 0.062 |
| 3 | 1.5 | 0.384 | 0.093 |
| 4 | 2.0 | 0.512 | 0.125 |
| 5 | 2.5 | 0.641 | 0.156 |
| 6 | 3.0 | 0.770 | 0.186 |
| 7 | 3.5 | 0.896 | 0.218 |
| 8 | 4.0 | 1.025 | 0.249 |

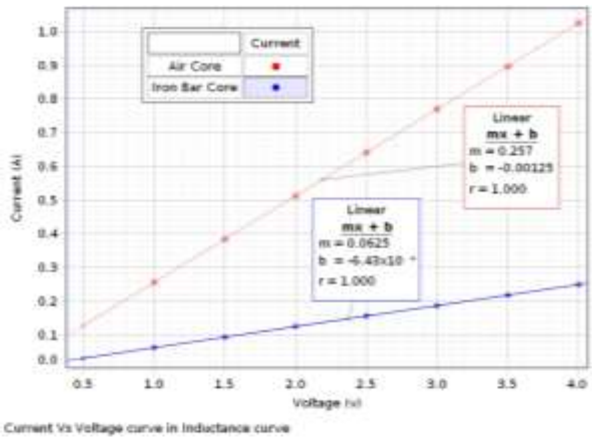


**Fig 2. Inductance results for air sample and Iron bar baseline**

Conducting the inductance test, all tested mixtures from Phases A and B, regardless of varying percentages of slag, iron fillings, and magnetite, did not exhibit any enhancement in magnetic properties. These mixtures aligned closely with the air sample line, indicating that the inclusion of these magnetic materials did not improve the magnetic properties compared to the air sample. Consequently, mixtures XIV, XV, XVI, and XVII in phase C were tested to further explore the potential improvements in their magnetic properties.

Figure 4 shows the baseline along with previously mentioned mixtures, illustrating their current versus voltage (I-V) characteristics. It can be concluded that a relationship exists between the electric current measured in amperes (A) and the voltage measured in volts (V). In this context, the slope of the line represents the reciprocal of the inductive reactance, expressed in 1/Ohm or siemens, given that inductive reactance is measured in ohms.

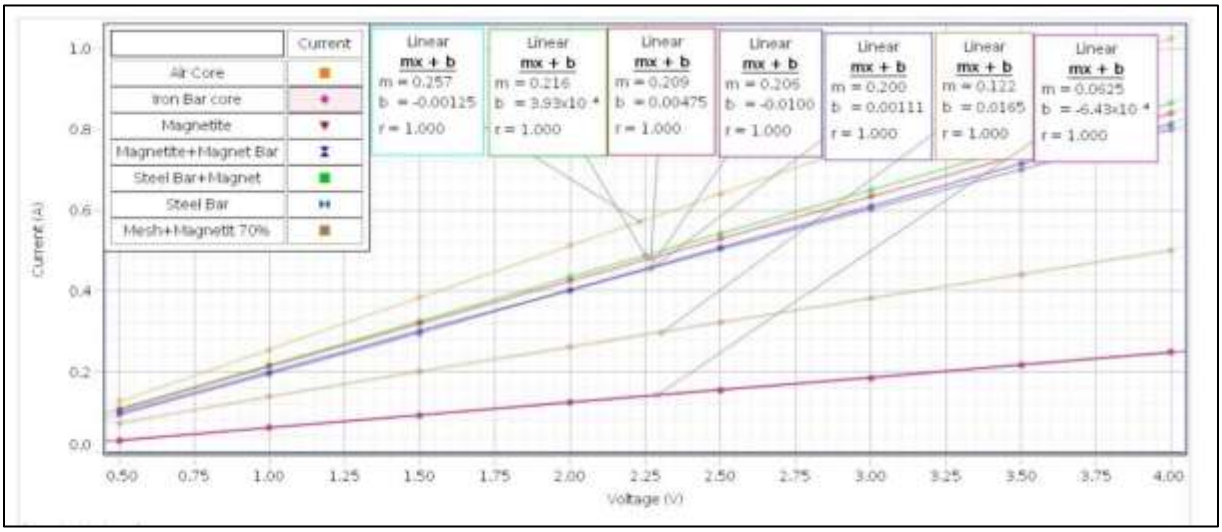


**Fig 3. Inductance results for all mortar mixtures**

The trendline slopes presented in Table 2 show the magnetic properties of the various mixtures. The air sample, serving as the baseline, has the highest slope of 0.257, indicating the lowest magnetic properties, while the iron bar, also a baseline reference, has the lowest slope of 0.062, signifying the highest magnetic properties. Among the tested mixtures, mixture XVII, which combines a steel bar and magnet, exhibits a slope of 0.216, the closest to the iron bar's baseline slope. This suggests that Mixture XVII possesses superior magnetic properties compared to other mixtures, making it a promising mixture for road applications requiring robust magnetic responsiveness. Other mixtures, such as mixture XIV, which includes magnetite and a magnetic bar, and mixture XV with a steel bar, also show improved magnetic properties with slopes of 0.206 and 0.200 (19.84-22.12% improvement), respectively. These results underscore the effectiveness of combining magnetic materials to approach the magnetic performance of the iron bar (Table 2).

**Table 2 Slope of all mixtures**

| Trendline (Description) | Slope |
|---|---|
| Air sample (Baseline) | 0.257 |
| Iron bar (Baseline) | 0.062 |
| Magnetite (Mixtures IV, V & VI) | 0.209 |
| Steel mesh and magnetite 70% (Mixture XVI) | 0.122 |
| Magnetite and magnetic bar (Mixture XIV) | 0.206 |
| Steel bar and magnet (Mixture XVII) | 0.216 |
| Steel bar (Mixture XV) | 0.200 |

Figure 5 serves as a conceptual illustration, showing how incorporating the enhancers with magnetic properties into the cement mortar mixtures exhibits sufficient magnetic properties to attract pieces of magnets on their own.

**Fig 4. Modified cement mortar with enhanced magnetic properties**

### *3.1.2. Magnetic Flux and Differential Permeability*

Based on the inductance test, the magnetic flux and differential permeability (μr) were calculated as it is a crucial parameter to evaluate the material's ability to become magnetized when exposed to a magnetic field. A higher differential permeability indicates better magnetic conductivity. As previously discussed in Figure 3, there was a direct relationship between the magnetic flux and differential permeability of the different mixtures.

Hence, the following equations were utilized:

$$X_L = \frac{1}{Slope} \text{ and } X_L = 2\pi f L, \text{ then } \frac{1}{Slope} = 2\pi f L \quad (1)$$

Where L is the inductance of the core material and measured in Henry (H), and ƒ is the frequency of the AC source and measured in Hertz (Hz).

$$L = \mu_O N^2 A / l \quad (2)$$

Where $\mu_o$ is the permeability of the air sample measured in Henry/m (H/m), A is the cross-section area of the core measured in meters squared ($m^2$), L is the length of the core measured in meters (m), and N is the number of turns of the coil.

Here N = 500 turns, A = 0.0016 $m^2$, L = 0.07 m, ƒ = 50 Hz, $\mu_o$ = 4 x 10-7 H/m

From the above, the inductive reactance can be calculated using the slope, the inductance can be calculated using Equation (1), and the permeability can be calculated from Equation (2).

Hence, the differential permeability $\mu_r = \frac{B}{\mu_o H}$

Where:

B = the magnetic flux density in Tesla (T) or milliTeslas (mT)

H = the magnetic field intensity in ampere per meter (A/m)

Mixture VI of phase A, which contained 70% magnetite, showed a $\mu_r$ of 1.97 and a B of 12.39 mT, which was inappropriate and inadequate to produce with it a wireless power transfer pad. As for mixture XVI, the stainless-steel mesh combined with 70% magnetite yielded the highest $\mu_r$ of 4.15 and the highest magnetic flux density of 26.10 mT.

### *3.2. Fresh Properties*

#### *Mini-Slump*

The mini-slump test for cement mortar mixtures were conducted based on a non-standardized method to evaluate mortar workability. The mini-slump values varied significantly across different mortar mixtures, influenced by factors such as the water-to-cementitious ratio (w/cm) and the inclusion of magnetic materials in varying percentages.

In Phase A, as illustrated in Table 3, the control mix, which was prepared without any magnetic materials, exhibited a mini-slump value of 165 mm. Mixtures containing 4% magnetite showed a slightly higher mini-slump value of 175 mm, indicating that while the presence of magnetite affects the mortar's workability, it did not lead to the highest workability among the mixtures. Notably, in Phase C, mixtures containing multiple additives were tested. Specifically, the mixture that incorporated 25% magnetite, 25% slag, and 70% iron fillings yielded a slump value of 192 mm, which was higher than the control mixture. This result indicated that the inclusion of these magnetic materials did not adversely affect the workability of the cement mortars (Table 3).

The data from Phase C demonstrated that the incorporation of significant percentages of magnetite, slag, and iron fillings not only enhanced the magnetization of the cement mortars but also improved their workability. Therefore, it can be concluded that the presence of these constituents enhances both the magnetic and workability properties of the cement mortars.

### *3.3. Hardened Properties*

#### *Compressive Strength*

The compressive strength of various mortar mixtures was measured according to ASTM C109 at intervals of 3, 7, and 28 days. These results demonstrated how different additives and modifications in the mixtures affect the compressive strength over time. Table 4 illustrates the varying compressive strength values at 3, 7, and 28 days for different mortar mixtures. Mixture I showed a consistent increase in strength from 3 to 28 days, indicating standard curing behavior without the influence of magnetic materials or special treatments. Mixture II showed a higher early strength at 3 days compared to the control but showed a less significant increase by 28 days, suggesting that the additives may accelerate early strength gain without substantially enhancing long-term strength. While mixture IV started with lower strength at 3 days but surpassed mixture I by 28 days. This indicates that magnetite may delay initial set or strength gain but contribute positively to the long term. Importantly, the compressive strengths for the mixture of phases C were 30 MPa and 38 MPa after 7 and 28 days. This result showed that with the addition of magnetite with a high percentage of 70% and slag and iron fillings up to 25%, the compressive strength was not affected negatively (Table 4).

**Table 3. Compressive strength at 3, 7 and 28 days**

| Mixture | Compressive Strength (MPa) | | |
|---|---|---|---|
| | 3 days | 7 days | 28 days |
| Phase A - Mixture I – Control Mixture | 27.8 | 32.9 | 40.0 |
| Phase A - Mixture II | 18.3 | 30.2 | 34.8 |
| Phase A - Mixture IV | 18.9 | 31.2 | 35.9 |
| Phase A - Mixture VII | 16.7 | 27.6 | 31.7 |
| Phase C - Mixtures XIV, XV, XVI, and XVII | 18.4 | 30.1 | 38.3 |

### *3.4. Durability*

### *3.4.1. Chemical Attack*

The chemical attack test, conducted according to ASTM C267, evaluated the durability of various mortar mixtures against chemical degradation over periods of 7 and 14 days. The detailed results of this assessment are presented in Table 5. The evaluation of chemical attack was concerned with measuring weight loss before and after exposure to sulfuric acid and the weight loss in percentages in brackets. All the mixtures showed minor weight loss and appropriate chemical soundness after 7 days with no significant difference. On the other hand, the chemical soundness after 14 days for other mixtures was different based on their constituents and percentages. Notably, the Phase C mixtures, which showed enhanced magnetic properties, displayed minimal weight loss, losing only 8 grams, which corresponds to 2.4%. This indicates superior durability in comparison to other mixtures.

**Table 4. Chemical soundness results**

| Mixture(s) ID | Initial Weight (g) | Weight after 7 days (g) (% Loss) | Weight after 14 days (g) (% Loss) |
|---|---|---|---|
| I | 292 | 288 (1.4%) | 277 (5.1%) |
| II | 292 | 281 (3.7%) | 274 (6.1%) |
| IV | 284 | 280 (1.4%) | 276 (2.8%) |
| VII | 285 | 281 (1.4%) | 272 (4.6%) |
| XIV, XV, XVI, and XVII | 338 | 334 (1.2%) | 330 (2.4%) |

The compressive strength of different mortar mixtures was measured after 14 days of chemical exposure to assess the impact on structural integrity. The results are illustrated in Table 6, showing how various additives influence compressive strength under chemical attack. For mixture I, the compressive strength decreased from 29.5 MPa to 25.20 MPa after 14 days, indicating a noticeable reduction in structural integrity due to chemical exposure. For mixtures within phase A, the addition of 10% slag showed a compressive strength decrease from 32.4 MPa to 24.12 MPa over 14 days, slightly better than the control mixture but still showing significant degradation. As for the addition of 4% magnetite, compressive strength was the highest initially at 33.8 MPa but dropped to 22.13 MPa, indicating that while magnetite reduced mass loss, it did not significantly protect against strength loss. The mixture that included 10% iron filings showed the most significant drop in compressive strength, from 37.9 MPa to 22.12 MPa, highlighting poor resistance to chemical attack. These results suggest that the inclusion of magnetite and a combination of additives may slightly mitigate weight loss in a chemical attack but not necessarily preserve compressive strength, indicating a complex interaction between material composition and chemical resistance (Table 6). These results demonstrated how different additives and modifications in the mixtures affect the compressive strength over time. Importantly, the mixture of phase C showed some reduction in compressive strength after 14 days of exposure to chemical attack.

**Table 5. Compressive strength after 14 days of exposure to chemicals**

| Mixture(s) ID | Compressive Strength (MPa) | |
|---|---|---|
| | 7 days | 14 days |
| I | 29.5 | 25.20 |
| II | 32.4 | 24.12 |
| IV | 33.8 | 22.13 |
| VII | 37.9 | 22.12 |
| XIV, XV, XVI, and XVII | 27.5 | 25.4 |

### *3.4.2. Abrasion Resistance*

The abrasion resistance test was conducted on various cement mortar mixtures to evaluate their durability against wear and tear, which is particularly important for pavement applications. The results of these tests are summarized below, with a focus on the performance of mixtures from different phases.

For the phase A mixtures, mixture I experienced an 8% weight loss, establishing a baseline for comparison. Similarly, the addition of 10% slag did not significantly impact abrasion resistance, as it also resulted in an 8% weight loss. This indicates that slag, at this percentage, does not enhance the abrasion resistance compared to the control. However, the mixture incorporating 4% magnetite demonstrated a notable improvement, with only a 2% weight loss. This substantial reduction suggests that magnetite significantly enhances the abrasion resistance of the mortar. As for the addition of 10% iron fillings, it results in 8% weight loss, similar to the mixture I and the slag-incorporated mixture. The results suggest that the inclusion of magnetite notably improves the abrasion resistance of mortar, with a significant decrease in weight loss observed in the mix containing 4% magnetite.

It was crucial to determine the abrasion resistance of the cement mortar mixture of phase C, which exhibited superior magnetic properties. The initial weight was 338 grams and yielded almost 1% weight loss after conducting the abrasion resistance test, in comparison to a weight loss of 8% in the control mixture. Therefore, it may be concluded that the incorporation of a high percentage of magnetite, slag, and iron fillings yielded a higher abrasion resistance than mixtures of phases A and B. This result is crucial for selecting materials for pavement applications, potentially extending the lifetime of the roads with lower maintenance and operation costs.

## 4. Conclusions

In light of the scope and based on the materials, procedures, and other parameters associated with this work, the following conclusions can be drawn:

- The incorporation of magnetite and scrap iron fillings as replacements for fine aggregates and slag as a replacement for Portland cement can lead to enhancement in the magnetic properties of cement mortars. However, the replacement of these magnetizable constituents should be in high percentages.
- The optimal magnetic properties were achieved in mixtures where fine aggregates were replaced by up to 25% magnetite and 70% scrap iron fillings, and Portland cement was replaced by up to 25% slag.
- Solely incorporating magnetite, slag, and iron fillings is insufficient to achieve desired magnetic properties. The addition of enhancers such as magnets, steel mesh, and steel bars is essential for substantial improvements.
- The mixtures incorporating high percentages of magnetite, slag, and iron fillings exhibited improved workability compared to the control mixture, indicating that these additions do not adversely affect the workability of cement mortars.
- The compressive strength of the all-portland cement mortars' mixtures showed a minor reduction in comparison to the control mixture. Importantly, the mixture of phase C that showed enhancement in magnetic properties had less compressive strength than the control mixture but still had adequate and appropriate compressive strength for road applications.
- The compressive strength of the mixtures post-chemical attack was lower than that of the control mixture, suggesting that further studies are needed to improve the chemical durability of these magnetizable mortars.

- The incorporation of a high percentage of magnetite, slag, and iron fillings yielded a higher abrasion resistance, which is an important parameter in selecting materials for pavement applications, than control cement mortars.
- This study represents a step on the way towards the introduction and implementation of rigid portland cement concrete pavement that possesses magnetizable properties. This coincides with the general trend of the promotion of electric vehicles to alleviate the negative impacts of conventional fuel-engine vehicles and reduce the harmful emissions.

## 5. Recommendations

As relatively little work has been conducted on this domain, the following recommendations can be made:

- The size gradation of magnetite and scrap iron fillings needs to be studied thoroughly to assess the gradation effect on the magnetic properties of portal and cement mortars.
- The economical aspect of these magnetizable cement mortars needs to be investigated to evaluate the different constituents and mixtures' design to yield more sustainable mortars.
- Statistically evaluating the fresh and hardened properties of mixtures containing 25% slag and 70% iron fillings.
- Investigating the magnetic properties of cement mortar utilizing natural magnetite and synthetic magnetite.
- Conducting more experimental tests for the mixtures, such as the water permeability and rapid chloride permeability tests.
- An extensive experimental work needs to be performed to study the corrosion resistance of these mortars, given their high content of iron, steel and ferrous materials. Also, the long-term impact of corrosion behavior on the compressive strength needs to be evaluated and assessed.
- More research studies are needed to understand the correlation between mechanical, magnetic and durability properties.
- The chemical reactivity properties and bonding characteristics between the different constituents need to be studied thoroughly for better durability of magnetized concrete.
- It is recommended to assess the carbon footprint for this magnetized concrete to evaluate its environmental advantage.
- A scanning electron microscope SEM and microstructural analysis are crucial to be conducted to assess the formation of different materials and for better understanding of the improvement of magnetic properties.

## 6. References

ASTM International. (2020). *ASTM C1437-20: Standard Test Method for Flow of Hydraulic Cement Mortar*. West Conshohocken, PA: ASTM International.

ASTM International. (2020). *ASTM C267-20: Standard Test Methods for Chemical Resistance of Mortars, Grouts, and Monolithic Surfacings and Polymer Concretes*. West Conshohocken, PA: ASTM International.

ASTM International. (2022). *ASTM A772/A772M-00(2022): Standard Test Method for AC Magnetic Permeability of Materials Using Sinusoidal Current*. West Conshohocken, PA: ASTM International.

ASTM International. (2023). *ASTM C1803/C1803M-23: Standard Guide for Abrasion Resistance of Mortar Surfaces Using a Rotary Platform Abraser*. West Conshohocken, PA: ASTM International.

ASTM International. (2024). *ASTM C109/C109M-24: Standard Test Method for Compressive Strength of Hydraulic Cement Mortars (Using 2-in. or [50-mm] Cube Specimens)*. ASTM International.

Bhagyashree, Panda, F. M. Rad, and M.S.Rajabi. (2023). Wireless Charing of Electric Vehicles Through Pavements: System, Design and Technology. *Handbook of Smart Energy SystemsEconPapers*.

Car and Driver. (2017). "BMW, Benz Hold Hands on Wireless Charging, Will Head to S-Class, i Cars." *Car and Driver*. Accessed January 15, 2025. *https://www.caranddriver.com/news/a15362624/bmw-benz-hold-hands-on-wireless-charging-will-head-to-s-class-i-cars*.

G.K. Glass, N.R. Buenfeld (2000). "The influence of chloride binding on the chloride induced corrosion risk in reinforced concrete." Corrosion Science 42, pages 329–344, https://doi.org/10.1016/S0010-938X(99)00083-9.

Hardman, S., Fleming, K. L., Khare, E., & Ramadan, M. M. (2021). A perspective on equity in the transition to electric vehicle. *MIT Science Policy Review* 2, 46-54.

International Energy Agency. *Global EV Outlook 2023: Trends in Electric Vehicle Markets and Implications for Road Transport.* https://www.iea.org.

Reza Tavakoli, A. Echols, U. Pratik, Zeljko Pantic. Fray Pozo, Amir Malakooti, Marc Maguire. (2017). Magnetizable Concrete Composite Materials for Road-Embedded Wireless Power Transfer Pads. *IEEE*

S.W. Tang, Y. Yao, C. Andrade, Z.J. Li (2015). "Recent durability studies on concrete structure". Cement Concrete Res. 78, pages 143–154, https://doi.org/10.1016/J.CEMCONRES.2015.05.021.

Schneider, K. Kamichi, D. Mikat, R. Sutton, M. Abdul-Hak, Y. Minagawa, H. Abeta, et al. (2018). "Bench testing validation of wireless power transfer up to 7.7kW based on SAE J2954." *SAE International Journal Passenger Cars Electron. Electr. Syst*. 11(2), 89–108.

Seixas Esteves, David. Joao Manuel da Fernandes Silva, Joana Diniz Fonseca, José Joaquim Poças Gonçalves, Filipe da Cerqueira Silva, Angela Maria de Jesus Sequeira Serra Nunes, Vitor Manuel Aires Vermelhudo, Diana Lara Matos Ferreira Tavares Correia, Joao Pedro Monteiro Serafim, (2022). *"Modified Mortar for Wireless Powered Lighting Systems*." Structural Concrete.

Soares, H. Wang. (2022). "A study on renewed perspectives of electrified road for wireless power transfer of electric vehicles". *Renewable Sustainable Energy Rev*. 158, 112110.

Tiemann, Myrel, Markus Clemens, and Benedikt Schmuelling. (2020). "Comparison of Conventional and Magnetizable Concrete Core Designs in Wireless Power Transfer for Electric Vehicles." *2020 IEEE PELS* Workshop on Emerging Technologies: Wireless Power Transfer, November 15-19, Seoul, Korea.

Yaowen, Pei, Feng Chen, Tao MA, Peng Peng, Gonghui, Yuxuan Ji (2023). "Towards a Novel Magnetic Asphalt Mixture Containing Ceramic Ferrites for Intelligently Encoding Road Traffic Sign Information." *Construction and Building Materials*.